Mass and volume transport variability in an eddy-filled ocean

CARL WUNSCH

Department of Earth, Atmospheric and Planetary Sciences, Massachusetts Institute of Technology, Cambridge, Massachusetts 02139, USA
e-mail: cwunsch@mit.edu

The possibility that the oceanic general circulation is undergoing changes as part, or the cause, of major climate shifts is being intensely discussed[1], with some published results relying on data from moorings spanning the North Atlantic Ocean[2,3]. The circulation is, however, extremely noisy. Here, I use existing estimates of the frequency and wavenumber content of geostrophic eddies in the ocean[4] to show that variations in ocean-wide integrated transport must appear even in the absence of a true long-term trend. Expected fluctuations exceed $\pm 20 \times 10^9\,\mathrm{kg\,s^{-1}}$ (or $\pm 20 \times 10^6\,\mathrm{m^3\,s^{-1}}$) and exhibit multi-year timescales. Existing knowledge of the eddy field allows predictions of observed variability and produces lower bounds on the (multi-decadal) timescale required to detect true trends of a large magnitude. Detecting and understanding the effect of climate change on the ocean circulation requires observations in three dimensions over long periods of time.

Until comparatively recently, the ocean circulation was viewed as consisting primarily of a large-scale, very slowly changing, flow. The discovery in the 1970s (ref. 5) of an intense field of variability, with mid-latitude spatial scales of 100 km and larger, and timescales of months and longer, greatly complicates efforts to discern long-timescale shifts in the basin-wide circulation. In particular, moorings deployed across the North Atlantic, as in the Rapid Climate Change Program (RAPID)[2,3,6] at 25° N, will produce apparent basin-scale mass transport trend-like variability, whose magnitude can be estimated *a priori*—the purpose here.

The ocean circulation is in near-geostrophic balance, meaning that there is an equilibrium between the Coriolis and pressure forces. An important peculiarity of this balance, heavily relied on by oceanographers, is that the total mass of fluid moving in the meridional overturning circulation (MOC) above any depth z_0, ocean-wide, depends only on the pressure difference across the basin—as long as bottom topography does not intervene above z_0. Thus, we need only observe pressure changes, for example, adjacent to the Bahamas on the west, and near the coast of Africa on the east, to determine fluctuations in the ocean circulation between those two places above the crest of the Mid-Atlantic Ridge (at about 2,000 m). Pressure data located between these two points are readily shown to 'drop-out' when computing the total meridional movement of water. More generally, and independent of method, zonally integrated meridional transport in geostrophic flows is extremely sensitive to end effects, whether the measurements are of pressure, or of velocity directly.

REPRESENTING THE EDDY FIELD

Oceanic variability can be characterized in many ways. Here, it is represented as a three-dimensional random field sufficiently near-gaussian to be depicted through its time mean (zero in all elements about a climatology) and a frequency–wavenumber power spectral density form proposed by Zang and Wunsch[4] (hereafter ZW). They constructed a spectral representation modulated by strongly spatially varying amplitude factors. See the Methods section for details.

Consider any moored system capable of measuring the temperature, T, and salinity, S, as a function of depth, z, and time t, at zonal position x and latitudinal position y. Then the pressure p at x, y, z, t can be obtained from hydrostatic balance as,

$$p(x,y,z_0,t) = g \int_{z_0}^{0} \rho(T(x,y,z,t), S(x,y,z,t), z)\,\mathrm{d}z + g\rho_0 \eta(x,y,t).$$

ρ is the fluid density as determined from temperature and salinity, g is the local gravitational acceleration and η is the displacement of the sea surface from the long-term mean. ρ_0 is a constant surface density. (x, y correspond to local cartesian zonal and meridional coordinates.) The mass transport, V, of fluid moving northwards above depth z_0, between two locations, x_1, x_2 with common latitude, y, is,

$$V(x_2 - x_1, y, z_0, t) \propto \int_{z_0}^{\eta} [p(x_2,y,z_0,t) - p(x_1,y,z_0,t)]\,\mathrm{d}z,$$

and above the bottom topography is not dependent on the values between x_1, x_2. The same equation applies both to the time mean and changes about that mean; only the variations are considered here. Temperature and salinity moorings do not produce measurements of the elevation changes, η, contributing to the pressure fluctuations. Three possibilities exist for inferring η. (1) Assume that at any instant, the value of η at the two locations conspires with the density field to produce a particular depth, z_c, where the pressure anomalies at x_1, x_2 are identical, producing a level of no horizontal motion—although there is no evidence for such behaviour. (2) Although such devices tend to drift, instruments measuring bottom pressure, p_b, can be placed at the sea floor and η can be deduced from p_b and temperature and
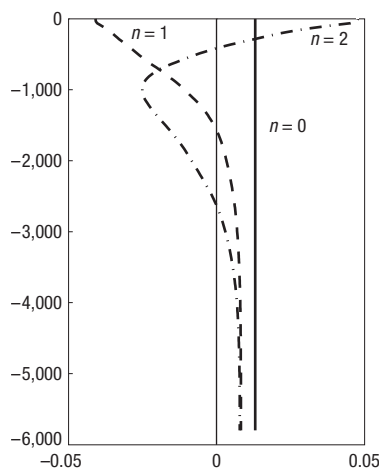
Figure 1 Barotropic ($n = 0$) and first two baroclinic ($n = 1, 2$) horizontal velocity and pressure modes[7] labelled $F_n(z)$, $n = 0, 1, 2, \ldots$, in the North Atlantic at 24° N, 32° W describing most variability. Notice that $n = 1$ has a zero crossing (level of no motion) at about 1,400 m. The approximate depth of the first zero crossing is a convenient reference integration depth, but any other depth can be used as long as no topography arises above that level. $n = 0$ is the barotropic mode, and has no measurable signature in temperature and salinity. Modal shapes vary slowly with position, and are normalized to integrate in the square to unity.

Figure 2 Simulation over 1,000 months (upper panel) of the transport variation between two moorings above about 1,000 m in which the eddy variability occurs incoherently. That behaviour is expected for any two moorings separated by more than about 30 km. The lower panel expands the upper one over a three-year time period. Extended intervals of apparent trends are visible, but are just the random superposition of eddy noise. These records have the mildly red spectral density assumed for the variability. (1 Sverdrup, Sv, is 10^6 m^3 s^{-1} $\approx 10^9$ kg s^{-1}.) No particular year or two is typical—long intervals of comparatively small and large transport occur.

salinity. (3) Altimetric satellites[7] are capable of direct measurements of η.

Altimetric data are by far the most abundant, and it is known[8] that the root-mean-square (r.m.s.) fluctuations of η in the western North Atlantic near the Bahamas are about 16 cm over timescales of several months, and on the eastern side, r.m.s. values are about 4 cm. Extensive current-meter mooring measurements in the ocean[9] have shown that η and ρ tend to co-vary. As a result, we can calculate flow characteristics as sums of the functions of depth, z, shown in Fig. 1—they are the oceanic vertical normal modes[9].

Given the altimetric measurements, and the assumption of the vertical structures, it is a simple matter, as outlined in the Methods section and Supplementary Information, to determine the frequency power density of the expected MOC transport and to produce examples of the sort of stochastic variations expected. Figure 2 shows a hypothetical realization of a transport curve, having the spectral density required for V. It was assumed that only vertical mode $n = 1$ was contributing and the transport values are for the region above $z_0 \approx 1,000$ m, slightly shallower than justified, and thus providing a lower bound on the total variability there. The so-called barotropic mode, with $n = 0$, has in practice about 50% of the eddy kinetic energy[9], but it is invisible in moored temperature and salinity measurements. (It is visible to the altimeters; it can also be inferred through the combination of measurements of temperature, salinity and bottom pressure.) The corresponding variability is just as real as that found from the other modes, but is not explicitly included here. Figure 2 can be compared to, for example, ref. 2, their Fig. 3, showing comparable changes from measurements. In practice, at 25° N in the Atlantic, further incoherent fluctuations of the Florida Current, which is confined there between Florida and the Bahama Islands, would have to be added to the variations plotted in Fig. 2 to determine the total fluctuations. A strong annual cycle in the surface layers is also not included here. These and other changes would need to be included in calculations of the transport of corresponding enthalpy (heat), freshwater and so on.
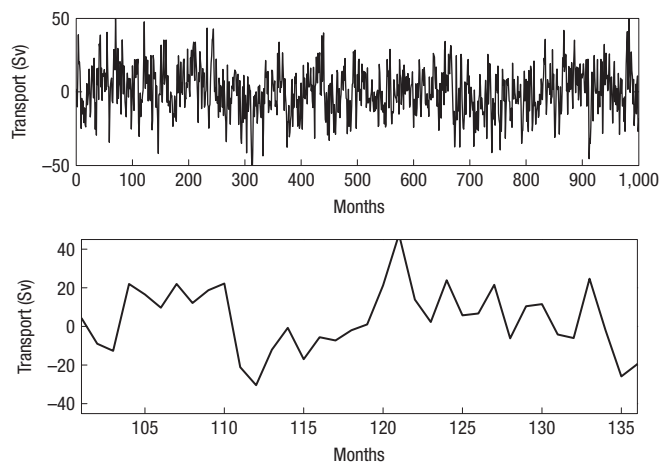
Even without $n = 0$, Fig. 2 shows changes with extremes approaching about 50×10^9 kg s^{-1}. For perspective, the time mean flow between the Bahamas and Africa is believed to be about 16×10^9 kg s^{-1} above about 1,000 m (ref. 10). Mass transport fluctuations about this value would be accommodated by water storage to the north and south, by compensating transport fluctuations below z_0 and by the Gulf Stream. The fluctuations seen in Fig. 2 are, in this example, wholly due to the random behaviour of an eddy field with an r.m.s. value of about 16 cm elevation change. It is immaterial whether the entire pressure variability occurs on the west, with the eastern mooring showing no change, or whether the corresponding incoherent pressure variances are partitioned between the moorings. As has been known for a long time[11], moored measurements of temperature (and by inference, salinity) decorrelate extremely rapidly with lateral separation of moorings; see Supplementary Information. Measurement intervals of a year or two are too short to draw inferences about the overall range of expected change—some years show little fluctuation, others very large values.

EXTENDED CONSIDERATIONS

The ZW spectral model is a simplified one, and produces an inter-mooring coherence (see the Supplementary Information) that is independent of frequency for all separations. Significant ocean variability is more complex than the gaussian random field so-described, including coherent and phase-locked vertical modes and probably also locked horizontal wavenumbers. Much more sophisticated and complete eddy (and even lower frequency), larger-scale motion representations can be constructed. It is difficult, however, to produce results that differ radically from the ones shown here, as long as the mooring measurements, or pressure determinations, are incoherent. Locally phase-locked disturbances can generate larger variations than estimated here, as the different vertical modes are likely to be reinforcing at least some of the

time. Modes for all n have finite amplitudes below the Mid-Atlantic Ridge crest and meridional transport variability can be calculated below the ridge crest in the eastern and western basins of the North Atlantic by using pressure field estimates from either side of the ridge along with those at the eastern and western edges. Again, we expect to see apparent trends—whose frequency structure is dependent on the spectrum of stochastic variability. Motions in the first baroclinic mode will tend to compensate[3] above and below the mode nodal line near 1,400 m, but the barotropic mode will not compensate, and higher modes, $n = 2, 3, \ldots$, will produce complicated amplification and cancellation as the vertical depth z_0 is shifted downward.

Using the present spectral representation, and the well-founded assumption that geostrophic balance applies, it is simple, using minimum variance estimation methods, to obtain the time required to detect a secular trend. As outlined in the Supplementary Information, it is found that a $2 \times 10^9 \, \mathrm{kg \, s^{-1} \, yr^{-1}}$ trend (a very large change) above about 1,000 m would require about 10 years of observations to become statistically significant at 95% confidence in the presence of the eddy field.

The full accuracy of the present spectral form is in doubt, because the values of the exponents, q, in the wavenumber power laws k^{-q} (see the Methods section) governing oceanic variability are subject to debate[12,13]; the ZW spectral representation was intended only as a place-holder, and could now be usefully re-evaluated. In particular, the altimetric record is now probably sufficiently long to justify modifying the frequency–wavenumber representation used by ZW. The low-frequency spectral slopes control the persistence time of MOC anomalies and thus the time to statistical significance of any given trend.

Well-tested eddy-resolving models with realistic eddy fields could be used to simulate observations independently of the calculations here. Most models used so far, however, do not resolve eddies at all or are at best only 'eddy-permitting'[14]. A least-squares fit of many data to a global general circulation model in the interval 1992–2004 showed much variability, but only very slight hints of trends in the North Atlantic mass transport[10]. That 1° horizontal spatial resolution did not support an eddy field, and thus the variability present in the results reflects, at best, the low-frequency, low-wavenumber (wavelengths greater than about 200 km) portion of the spectra used here, and underestimates the total apparent transport fluctuations.

Separating true trends from eddy random walks as seen here, is a considerable challenge. The near-continuous spatial coverage provided by altimetric missions, and the spatially sparse but near-time-continuous Argo-float coverage, combined with high-resolution general circulation models, probably provide the best method for suppressing the eddy contributions. If changes are seen, whatever the cause, then we must try to understand them. Geostrophic transport calculations, inevitably sensitive to zonal end-point data as discussed here, will require very long times to produce statistically significant trends in the presence of an intense and ubiquitous eddy field. Noise reduction by spatial averaging moorings is very difficult. Strategies for doing better are clear: an understanding of the complete (three-dimensional) space–time structure of the variability, including particularly its latitudinal extent, can produce much more robust inferences. The eddy field will decorrelate meridionally, and detected trends that extend hundreds to thousands of kilometres both zonally and meridionally can be attributed to physics other than eddy noise. An understanding of causes and consequences of such trends will also involve far more than local physics. Changes perceived at any particular latitude are unlikely to be solely the consequence of local forcing changes. It is characteristic of fluids that perturbations having taken place in the distant past and in sometimes far-distant regions can be propagated over long distances, even globally: the ocean circulation has memory elements from seconds out to many thousands of years.

The ocean and climate communities need to move towards observing systems and models that are both truly global, and capable of long-term and long-distance integrations. Such models exist today, and prototypes of the requisite global observations lie with the satellites (altimetry, scatterometry, gravity and so on) and the Argo-float type of unmanned observations[10]. Ocean physics and related climate physics are global phenomena of long duration, and can only be understood with global information. 'Real-time' detection of secular changes in the oceanic overturning circulation by regional measurements is probably a mirage.

METHODS

BASIC SPECTRAL FORM

Following ZW, oceanic pressure variability, p, can be represented in a spatially separated form as,

$$p(x, y, z, t) = \sum_{n=0}^{\infty} p_n(x, y, z, t) = \sum_{n=0}^{\infty} P(x, y, t, n) F_n(z).$$

x, y, z being local cartesian coordinates, with z positive upward, x zonal, y meridional (ZW used spherical coordinates), and $F_n(z)$ is a vertical mode derived from standard separation of variables and solution of a Sturm–Liouville problem. $n = 0$ represents the flat-bottom ocean barotropic (uniform horizontal velocity) mode, and $n = 1, 2, \ldots$ are the baroclinic modes of Fig. 1. Assume the modes all vary independently, and p to be a zero-mean near-gaussian random field.

In analogy to the internal wave case[15], define the local three-dimensional Fourier representation as,

$$P(x, y, t, n) = \iiint_{-\infty}^{\infty} \hat{p}(k, l, \omega, n) \exp(2\pi i (kx + ly - \omega t)) \, \mathrm{d}k \, \mathrm{d}l \, \mathrm{d}\omega,$$

where k, l, ω are angular and not radian variables. Then up to a normalizing factor, the power density spectrum of P is, locally,

$$\langle \hat{p}(k, l, \omega, n) \hat{p}(k, l, \omega, n)^* \rangle = \Phi(k, l, \omega, n),$$

with $*$ denoting the complex conjugate. Brackets denote the theoretical expected value. $\Phi(k, l, \omega, n)$ is written in the separable form,

$$\Phi(k, l, \omega, n) = B_n(k) C_n(l) D_n(\omega) E_0(n), \qquad (1)$$

where in practice, ZW had inadequate information to distinguish any n dependence of B, C, D, and these indices are suppressed below. All modes thus have the same frequency–wavenumber structure. $E_0(n)$ represents the energy proportion of mode n, so that[4,9] $E_0(0) = 1$, $E_0(1) = 1$, $E_0(2) = 1/2, \ldots$ ZW then assumed, $C(k) = B(k)$—a limited form of horizontal isotropy, leading the meridional and zonal velocities to have the same power density spectrum. None of these assumptions is likely to be strictly accurate, but without further information, there is no reason to construct a more complex form.

A piecewise linear power-law form is,

$$
\begin{aligned}
D(\omega) &= \alpha_1 \omega^{-1/2}, \quad 0 < \omega \le 1/3.3 \text{ months} \\
&= \alpha_2 \omega^{-2}, \quad 1/3.3 \text{ months} < \omega, \\
B(k) &= C(k) = \beta_1 k^2, \quad 0 < k \le 1/40{,}000 \text{ km} \\
&= \beta_2 k^{-1/2}, \quad 1/40{,}000 \text{ km} \le k \le 1/400 \text{ km} \\
&= \beta_3 k^{-5/2}, \quad 1/400 \text{ km} \le k
\end{aligned}
$$

where α_i, β_i are constants that render the results continuous in ω, k. Choosing

$$\int_{\omega_{\min}}^{\omega_{\max}} D(\omega) \, \mathrm{d}\omega = \int_{k_{\min}}^{k_{\max}} B(k) \, \mathrm{d}k = 1$$

where the limits will be the prescribed limits of the frequency (one cycle in 10 years to 1 cycle/month) and wavenumber bands (1 cycle/10,000 km to 1 cycle/10 km) of interest here.

An external scale factor, A_n, is defined such that

$$F_n(0)^2 \iiint_{-\infty}^{\infty} \Phi(k, l, \omega, n) \, \mathrm{d}k \, \mathrm{d}l \, \mathrm{d}\omega$$

$$= A_n^2 F_n(0)^2 \iiint_{-\infty}^{\infty} B(k)B(l)D(\omega) \, \mathrm{d}k \, \mathrm{d}l \, \mathrm{d}\omega$$

$$= A_n^2 F_n(0)^2$$

is the mean-square surface pressure variation in the variability.

Here, I use the surface value of $F_1(0) \approx 0.05$ in the empirical mode shown in Fig. 1. The final form of equation (equation (1)) is thus,

$$\Phi(k, l, \omega, n) = A_n^2 B(k)B(l)D(\omega),$$

with $B(k)D(\omega)$ as plotted by ZW.

A SIMULATED RECORD

A spatial pressure difference at the sea surface of $\Delta\eta = 1$ cm at 25° N generates a transport variation/unit depth of,

$$V \approx \frac{g\rho_0}{f} \Delta\eta = 1.7 \times 10^6 \ \mathrm{kg\,s^{-1}\,m^{-1}}.$$

The zero crossing of horizontal velocity in mode $n = 1$ is below about 1,000 m depth and treating the area simply as a triangle above that depth (Fig. 1) representing mode $n = 1$ alone, gives $V \approx 8.3 \times 10^8 \ \mathrm{kg\,s^{-1}}$ above 1,000 m. Thus, 16 cm r.m.s. produces about $16 \times 10^9 \ \mathrm{kg\,s^{-1}}$ of variation. On the eastern side of the North Atlantic at this latitude the altimetric variability is about 4 cm r.m.s., or taking a total variance of $16^2 + 4^2$, implying about $270 \times (10^9 \ \mathrm{kg\,s^{-1}})^2$ for the transport variability, thus defining A_1, and noting that there is no difference between assuming that all of the variability occurs at one of the moorings, or partitioning it incoherently between two of them. It is straightforward to generate a stationary gaussian time series whose power density is known[16,17]. Figure 2 shows a realization of the transport variation having the power density spectrum $\Psi_t(L/2, 0, \omega, n)$ of transport, and is discussed in the Supplementary Information. As the incoherent motions at the two end points go randomly

in and out of phase, reinforcement and cancellation of the local transport fluctuations occurs.

References

1. Schiermeier, Q. Gulf Stream probed for early warnings of system failure. *Nature* **427**, 769 (2004).
2. Cunningham, S. A. *et al*. Temporal variability of the Atlantic meridional overturning circulation at 26.5° N. *Science* **317**, 935–938 (2007).
3. Kanzow, T. *et al*. Observed flow compensation associated with the MOC at 26.5° N in the Atlantic. *Science* **317**, 938–941 (2007).
4. Zang, X. & Wunsch, C. Spectral description of low frequency oceanic variability. *J. Phys. Oceanogr.* **31**, 3073–3095 (2001).
5. MODE Group. The mid-ocean dynamics experiment. *Deep-Sea Res.* **25**, 859–910 (1978).
6. Rayner, D. (ed.) *RRS Discovery Cruises D277/D278, RAPID Mooring Cruise Report, February–March 2004* (SOC Cruise Report 53, Southampton UK, 2005).
7. Fu, L.-L. & Cazenave, A. (eds) *Satellite Altimetry and Earth Sciences. A Handbook of Techniques and Applications* (Academic, San Diego, 2001).
8. Wunsch, C. & Stammer, D. Satellite altimetry, the marine geoid and the oceanic general circulation. *Ann. Rev. Earth Planet. Sci.* **26**, 219–254 (1998).
9. Wunsch, C. The vertical partition of oceanic horizontal kinetic energy. *J. Phys. Oceanogr.* **27**, 1770–1794 (1997).
10. Wunsch, C. & Heimbach, P. Decadal changes in the North Atlantic meridional overturning and heat flux 1993–2004. *J. Phys. Oceanogr.* **36**, 2012–2024 (2006).
11. Richman, J., Wunsch, C. & Hogg, N. Space and timescales of meso-scale motion in the western North Atlantic. *Rev. Geophys. Space Phys.* **15**, 385–420 (1977).
12. Stammer, D. On eddy characteristics, eddy mixing and mean flow properties. *J. Phys. Oceanogr.* **28**, 727–739 (1997).
13. Scott, R. B. & Arbic, B. K. Spectral energy fluxes in geostrophic turbulence: Implications for ocean energetics. *J. Phys. Oceanogr.* **37**, 673–688 (2007).
14. Ganachaud, A. Error budget of inverse box models: The North Atlantic. *J. Atmos. Ocean. Technol.* **20**, 1641–1655 (2003).
15. Garrett, C. J. R. & Munk, W. H. Space–timescales of internal waves. *Geophys. Fluid. Dyn.* **3**, 225–264 (1972).
16. Percival, D. B. Simulating Gaussian random processes with specified spectra. *Comput. Sci. Statist.* **24**, 534–538 (1992).
17. Wunsch, C. The interpretation of short climate records, with comments on the North Atlantic and Southern Oscillations. *Bull. Am. Met. Soc.* **80**, 245–255 (1999).